NUMERICAL INVESTIGATION OF SUPERSONIC VISCOUS GAS FLOW OVER LONG BLUNT CONES WITH ALLOWANCE FOR EQUILIBRIUM PHYSICOCHEMICAL EFFECTS

S. V. Utyuzhnikov

UDC 533.6.011.8:519.63

Supersonic axisymmetric viscous heat-conducting gas flow over long spherically blunted cones is considered over a broad range of Reynolds numbers on the basis of the complete system of viscous shock layer equations. An economical numerical method based on global iterations is used to solve the viscous shock layer equations. The general influence of the second-approximation effects of boundary layer theory and the influence of equilibrium physicochemical processes on the heat loads are determined for bodies with a large aspect ratio.

In order to calculate numerically gas flow over long bodies we will use the complete system of equations of a viscous shock layer (see, for example, [1]). In the curvilinear coordinate system x, y tied orthogonally to the body, this system contains all the terms of the complete Navier—Stokes equations which contribute to the second approximation of asymptotic boundary layer theory for both the inner and outer expansions. As one of the boundaries of the solution domain we will take the detached bow shock, whose position is determined in the course of solving the problem. On the shock wave we impose the generalized Rankine—Hugoniot conditions [1].

A comparison of the numerical solutions of the complete Navier—Stokes equations and the viscous shock layer equations, which had previously been made only for relatively short bodies (see, for example, [2, 3]), showed that for fairly smooth bodies (without a discontinuity in the angle of inclination of the generator) the viscous shock layer model gives good accuracy with respect to determination of the values of the pressure, friction and heat flux on the surface of the body up to $\mathrm{Re}_\infty \sim 100$, i.e., even for a perfectly viscous shock layer, when formally the equations are not asymptotically correct. In this case the maximum error in determining the aerodynamic and thermal loads on the body is about 1% when $\mathrm{Re}_\infty > 10^3$ and about 10% when $\mathrm{Re}_\infty \sim 10^2$. Our aim was to investigate the flow over bodies with a large aspect ratio on the basis of the viscous shock layer equations.

1. NUMERICAL METHOD OF SOLUTION

The viscous shock layer equations preserve the elliptical properties of the problem in subsonic flow regions (see, for example, [3, 4]). Moreover, in the blunt-end zone in order to determine the position of the shock wave at a given point it is necessary to take into account the transmission of information upstream [3], in which the "ellipticity" of the problem is also expressed.

In order to solve the system of viscous shock layer equations we will use a method based on global iterations [3, 5]. In each global iteration the value of the tangential component of the pressure gradient is determined from the relation

$$\frac{\partial p^{(n+1)}}{\partial x} = \alpha_t \frac{\partial p_t}{\partial x} + (1 - \alpha_t) \frac{\partial p_g^{(n)}}{\partial x}, \quad 0 \le \alpha_t \le \frac{u^2}{a^2}$$

where $\partial p_t/\partial x$ is the part of the pressure gradient which is determined on the basis of the calculation of the current $(n+1)$-th global iteration, $\partial p_g/\partial x$ is the part of the gradient determined on the basis of the calculation of the preceding iteration, u is the velocity vector component tangential to the body, and a is the local speed of sound.

In each global iteration the Cauchy problem in x for the viscous shock layer equations is properly posed. In order to approximate derivatives of the type $\partial p^{(n)}/\partial x$ the point on the difference grid that stands in front is used. Moreover, in the blunt-end zone in each global iteration the position of the shock wave is determined on the basis of the calculation of the previous iteration.

For calculating the flow over long bodies we used a block-marching realization of the method proposed in [6]. In this approach the entire calculation domain is divided with respect to x into mutually intersecting subdomains (blocks). Starting from

Moscow. Translated from Izvestiya Rossiiskoi Akademii Nauk, Mekhanika Zhidkosti i Gaza, No.1, pp. 202-205, January-February, 1993. Original article submitted May 27, 1991.

0015-4628/93/2801-0155$12.50

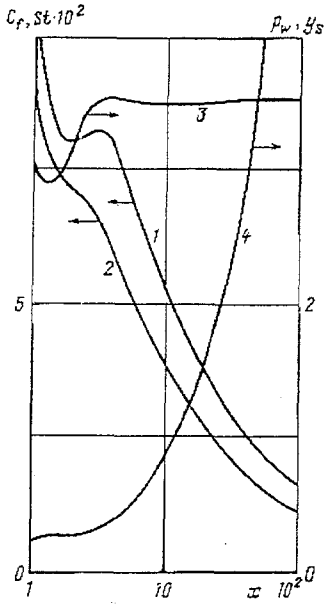

Fig 1

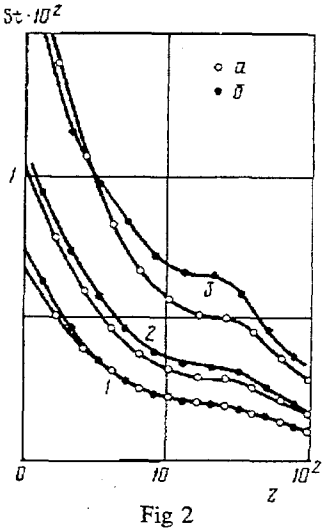

Fig 2

the second block, outside the blunt-end zone, the position of the shock wave can be determined in the course of calculating the current block. This approach makes possible considerable economies in computer memory and machine time.

For the numerical solution of the system of equations in each global iteration we used a different scheme with an enhanced order of approximation [5], which was second-order accurate in the longitudinal coordinate and fourth-order accurate in the transverse coordinate. Moreover, in the transverse direction we constructed a difference grid adaptive to the solution [7]. In the longitudinal direction we used a variable step, which was assigned before solving the problem.

For calculating the gas flow over a cone with a length equal to 200 bluntness radii R_w we used 4—5 blocks with a 120×40-point total grid. A typical flow time with convergence to 1% over the entire pressure field was 20—30 min on a BÉSM-6 computer; calculating the first block required 5—7 global iterations and calculating the subsequent blocks 2—4 iterations.

2. RESULTS OF THE CALCULATIONS

Figure 1 shows the distribution of the local friction coefficient $C_f = \mu \partial u/\partial y (\rho_\infty V_\infty^2/2)^{-1}$ (curve 1), the Stanton number $St = q_w/(\rho_\infty V_\infty H_\infty)$ (curve 2), the pressure on the body divided by $\rho_\infty V_\infty^2/2$ (curve 3), and the shock wave standoff distance divided by R_w (curve 4) for the case of flow over a cone with spherical bluntness and a half-angle $\theta = 35°$ for $M_\infty = 15$, $\gamma = 1.4$, $Re_\infty = 10^3$, $T_w = 0.05$. Here and everywhere in what follows, the basic notation is that usually employed, and the Reynolds number Re_∞ is determined from the free-stream parameters and the blunt-end radius.

It is interesting to note that in the region of the pressure "spoon" there is a local maximum of the friction coefficient. This effect is observed for fairly large cone angles (>30°), but in all cases the pressure "spoon" leads at least to the formation of a friction and heat flux "shelf."

In addition to modeling a perfect gas flow with constant γ we investigated the effect of equilibrium physicochemical processes on the heat flux. For calculating the transport coefficients of the air we used tables compiled by S. A. Vasil'evskii and I. A. Sokolova. Figure 2 gives the heat flux distribution along the descent trajectory of a spherically blunt cone in the earth's atmosphere ($R_w = 1$ cm, $\theta = 10°$, $T_w = 500°$). Here and in what follows, z corresponds to the axial coordinate reckoned from the vertex of the cone and divided by R_w.

Curves *a* correspond to the heat flux distributions for a polytropic gas (with constant specific heat) and curves *b* to those for chemical-equilibrium air at the same values of M_∞ and Re_∞. Curves 1 correspond to an altitude $H = 50$ km and a flight velocity $V = 3$ km/sec, curves 2 to $H = 55$ km and $V = 5$ km/sec, and curves 3 to $H = 60$ km and $V = 7$ km/sec. With fall in the temperature of the gas during its motion downstream in the shock layer the corresponding curves approach each other, and at the lower point of the trajectory (curve 1) coincide. The maximum difference in the heat fluxes corresponds to the region of the pressure "spoon." At the lower point of the trajectory the zone of maximum difference in the heat fluxes is displaced into the region of the junction between the sphere and the cone. From an altitude of approximately 45 km and below the air throughout the shock layer can be regarded as a polytropic gas.

The variation of the effective specific heat ratio γ and the temperature in the shock layer for the mid-point of the trajectory

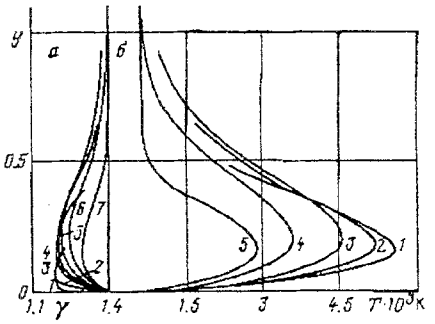

Fig 3

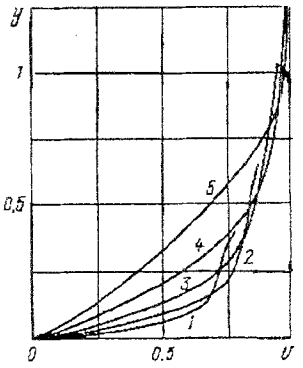

Fig 4

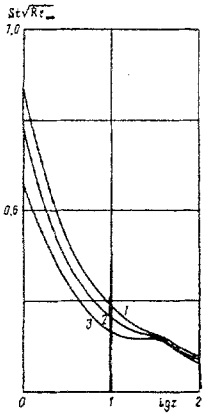

Fig 5

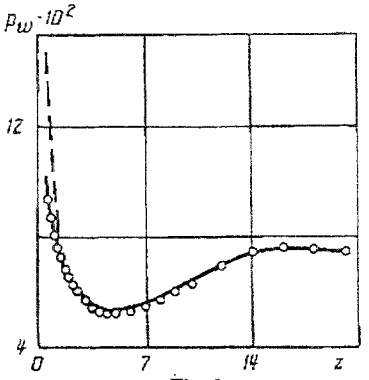

Fig 6

is shown in Fig. 3. Curves 1—7 (*a*) correspond to $z=0$, 0.6, 1, 2, 3, 9, and 12. On the cold wall $\gamma=1.4$. As was to be expected, in the high-temperature region γ takes minimum values. For fairly large z the gas in the inviscid flow region may be regarded as polytropic with $\gamma=1.4$. In this region the temperature of the gas is close to the temperature of the wall. The temperature profiles 1—5 (*b*) correspond to $z=1.36$, 2, 3.9, 12, and 41.

In Fig. 4 we have plotted the profiles of the tangential velocity component divided by the free-stream velocity for a cone with $\theta=10°$ when $M_\infty=20$, $Re_\infty=3\cdot10^3$, and $T_w=0.026$. Curves 1—5 correspond to the sections $x=$const with $x=0.83$, 1.5, 3.4, 12, and 100 (in lengths R_w). With increase in x the profiles become more and more full. Outside the boundary layer for large values of x (of the order of $100R_w$ and more) the flow is almost uniform.

Since the complete viscous shock layer equations are solved over the entire region of flow between the bow shock and the surface of the body, the second-approximation effects of boundary layer theory are automatically taken into account. Comparison with the classical boundary layer asymptotics, corresponding to $Re_\infty\to\infty$, enabled us to estimate the total contribution of the second-approximation effects.

In Fig. 5 we have plotted the heat flux distribution along the surface of a cone with spherical bluntness ($\theta=10°$, $M_\infty=20$, $T_w=0.5$). Curves 1—3 correspond to the values $Re_\infty=3.1\cdot10^3$, 10^4, and 10^6. The difference in the curves according to the Reynolds number is attributable to the influence of second-approximation effects. The maximum difference corresponds to the region of the pressure "spoon." On the cold wall ($T_w=0.025$) the difference between the analogous curves is much less and amounts to 15—20%. It should be noted that although the vortex interaction effect has a strong influence on the heat flux [6], the total contribution of the second-approximation effects is much lower.

Figure 6 shows the pressure distribution along the surface of a cone with $\theta=15°$ traveling at $H=30$ km and $V=15$ km/sec when $Re_\infty=6\cdot10^5$. The points represent the data of [9] corresponding to ideal gas flow. The broken curve represents calculations made by a marching method [10] with regularization of the Cauchy problem. In the case under consideration this approach introduces a significant error over a distance of up to two bluntness radii, mainly where there is an extensive subsonic region. Further downstream the second global iteration introduces an unimportant change into the marching calculations and is more necessary for checking the accuracy of the latter. The pressure values calculated from the viscous shock layer model are in good agreement with the values for ideal gas flow.

The author wishes to thank S. A. Vasil'evskii and I. A. Sokolova for providing the tables used to calculate the transport coefficients and G. A. Tirskii for his constant interest and useful discussions.

REFERENCES

1. É. A. Gershbein, S. V. Peigin, and G. A. Tirskii, "Supersonic flow past bodies at low and intermediate Reynolds numbers," in: *Advances in Science and Engineering. All-Union Institute of Scientific and Technical Information. Fluid Mechanics*, Vol. 19 [in Russian] (1985), p. 3.
2. N. S. Kokoshinskaya, B. M. Pavlov, and V. M. Paskonov, *Numerical Modeling of Supersonic Viscous Gas Flow Past Bodies* [in Russian], Izd. MGU, Moscow (1980).
3. S. V. Utyuzhnikov, "Numerical method of solving the complete viscous shock layer equations," *Abstract of Thesis for the Degree of Candidate of Physico-Mathematical Sciences* [in Russian], Moscow Physico-Technical Institute (1986).
4. V. I. Timoshenko, *Supersonic Viscous Gas Flows* [in Russian], Naukova Dumka, Kiev (1987).
5. S. A. Vasil'evskii, G. A. Tirskii, and S. V. Utyuzhnikov, "Numerical method of solving the viscous shock layer equations," *Zh. Vychisl. Mat. Mat. Fiz.*, **27**, 741 (1987).
6. S. V. Utyuzhnikov, "Numerical solution of the complete viscous shock layer equations in the blunt body hypersonic flow problem" *Chisl. Metody. Sploshnoi Sredy*, **17**, 125 (1986).
7. S. A. Vasil'evskii and G. A. Tirskii, "Effect of multicomponent diffusion and higher approximations for the transport coefficients on the heat transfer in hypersonic blunt body flow," in: *Applied Problems of Aircraft Aerodynamics* [in Russian], Naukova Dumka, Kiev (1984), p. 100.
8. Yu. G. El'kin, Yu. N. Ermak, I. I. Lipatov, and V. Ya. Neiland, "Blunt cone entropy layer absorption in hypersonic viscous gas flow," *Uch. Zap. TsAGI*, **14**, 18 (1983).
9. V. V. Lunev, K. M. Magomedov, and V. G. Pavlov, *Hypersonic Flow Past Blunt Cones with Allowance for Equilibrium Physicochemical Processes* [in Russian], Computer Center of the USSR Academy of Sciences, Moscow (1968).
10. V. M. Kovenya and S. G. Chernyi, "A marching method for solving steady simplified Navier—Stokes equations," *Zh. Vychisl. Mat. Mat. Fiz.*, **23**, 1186 (1983).